HHS Public Access

Author manuscript

Connect Tissue Res. Author manuscript; available in PMC 2019 December 01.

Published in final edited form as:

Connect Tissue Res. 2018 December ; 59(SUP1): 102–110. doi:10.1080/03008207.2017.1409219.

Novel Insights into Renal Mineralization and Stone Formation through Advanced Imaging Modalities

Scott V Wiener, MD, **Ling Chen, PhD**, **Alex R Shimotake**, **Misun Kang, PhD**, **Marshall L Stoller, MD**, and **Sunita P Ho, PhD**

Sunita P Ho, Ph.D., Professor, Department of Urology, School of Medicine, Professor, Department of Preventive and Restorative Dental Sciences, School of Dentistry, University of California San Francisco

Abstract

Purpose/Aim: The most common kidney stone composed of calcium oxalate forms on interstitial calcium phosphate mineral known as a Randall's plaque. Due to limited information about events leading to the initial deposition of nanometer size interstitial calcium phosphate pre-clusters, there continues to be a debate on the initial site of calcium phosphate deposition and factors leading to stone formation.

Materials and Methods: High-resolution micro-CT, and light and electron microscopy techniques were used to characterize human renal pyramids and five representative kidney stones with identifiable stems. Mineral densities of mineralized aggregates within these specimens were correlated with micro- and ultra-structures as seen using light and electron microscopy techniques.

Results: The earliest detectable biominerals in the human renal papilla were proximal intratubular plate-like calcium phosphate deposits. Unoccluded tubules were observed by electron microscopy and micro-CT in stems connected to calcium phosphate stones. These tubules were similar in diameter (30 – 100 μm) and shape to those observed in the distal regions of the renal papilla.

Conclusions: Observations were patterned through a novel and unified theory of stepwise-architecture guided biomineralization (a combination of smaller structures leading to a larger but similar structural framework). A plausible stepwise progression in renal biomineralization is proposed; proximal intratubular calcium phosphate deposits can lead to interstitial yet calcium phosphate rich Randall's plaque and mature into a stem on which a calcium oxalate stone grows within the collecting system of a kidney.

Keywords

kidney stone; biomineralization; Randall's plaque; micro-CT; correlative microscopy

Corresponding Author: 707 Parnassus Avenue, D 3212, School of Dentistry, University of California, San Francisco, San Francisco, CA 94143 Health Sciences West (HSW) 813, 513 Parnassus Avenue. University of California, San Francisco, San Francisco, CA 94143, sunita.ho@ucsf.edu, Phone: 415-514-2818, Fax: 415-476-0858.

Declaration of Interests: The authors report no financial conflicts of interest.

1. INTRODUCTION

Kidney stones, or nephrolithiasis, are a common condition affecting approximately one in eleven individuals in the United States of America, and are becoming even more prevalent with an increase in diabetes and obesity [1]. Seventy percent of all calculus and stones are predominantly calcium oxalate crystals [2]. Stones generally form within the renal collecting system, and are attached to a calcium phosphate lesion of the renal papilla known as the Randall's plaque (RP). Alternatively, stones may sometimes form as part of a plug in the duct of Bellini (due to hyperoxaluria and distal tubular acidosis, often in patients who have undergone gastric bypass) or in free solution (such as in cystinuria) [3]. The current study will focus on the classic mechanism of calcium oxalate nucleation onto RP. Mineralized lesions of the kidney such as RP fall into a category termed nephrocalcinosis, in contrast to stones within the renal pelvis and ureter which are categorized as nephrolithiasis.

In 1937, Alexander Randall first described RP in 17 percent of the examined cadaveric kidneys [4]. Later, Anderson and colleagues identified microscopic calcifications throughout the papilla and felt that these may even represent a normal physiologic process [5]. Subsequently, Carr detected these calcifications radiographically and proposed a lymphatic mechanism for their deposition and propagation [6]. The theories of Anderson, Carr, and Randall were synthesized by Bruwer into a stepwise dogma known as the Anderson-Carr-Randall progression where these microscopic calcifications would migrate by lymphatic fluid-flow from the proximal papilla to the distal interstitium to become RP [7]. However, causative evidence linking proximally observed intratubular mineralization to distal interstitial RP in support of the Anderson-Carr-Randall Progression is yet to be identified.

Over the past several decades, multiple attempts to describe the inciting event of RP formation and subsequent stone growth have been undertaken. Much research and interest has focused on the interstitial area where plaque is found, while novel imaging modalities with higher resolving capacities have begun to shed light on previously undescribed upstream minerals [8–11]. A causative relationship between mineral formation in the proximal tubules within the renal papilla and ultimately the large-scale stone in the renal collecting system has not been shown. In this study, a new theory on the development and progression of the RP into a fully formed stem followed by formation of a kidney stone is presented along with insights into potential site-specific targeted pharmacological intervention. Results will illustrate semi-quantitative maps of site-specific concretions within the human renal papillae commonly of a pyramidal shape to provide insights into the structure and mineral density variations of the site-specific biominerals. Additionally, a theory that would link the proximal biominerals with the commonly observed distal interstitial RP, stems, and subsequently the stones is also discussed.

2. MATERIAL AND METHODS

2.1. Specimen Preparation

The UCSF Committee on Human Research Protection Program, IRB # 14–14533, provided authorization for the collection of human renal pyramids at the time of nephrectomy in the course of routine clinical care. More than 30 human papillae were excised at the time of

nephrectomy and fixed in formalin. Specimens were included if the underlying pathology did not distort the normal gross architecture of the renal pyramid as determined by the surgeon. Renal pyramids from kidneys with a history of chronic stone formation, chronic infection, hydronephrosis/obstruction, and/or cystic kidney disease were excluded due to distortion of the normal anatomy. Renal pyramids were placed in formalin and all specimens were examined for RP using a stereomicroscope and categorized as RP positive or negative by the presence of visible plaque within the subsurface layers of the distal one-third of the renal pyramid.

Stones were obtained under the same IRB protocol from patients undergoing percutaneous nephrolithotomy or ureteroscopy. Out of a catalogue of over 500 stones, five specimens representative of the population of stones with stems were selected for detailed analyses. Stone visually appeared to be unfragmented and previously attached to the renal papilla via an intact and identifiable stem. Specimens were sterilized using 0.31 Mrad of gamma radiation prior to imaging [12].

2.2. Micro-CT and Mineral Density Evaluation

Renal pyramids from kidneys were scanned at 4X magnification under wet conditions using a high-resolution X-ray micro-computed tomography (Micro XCT-200, Carl Zeiss Microscopy, Pleasanton, CA) unit. Stone specimens were also scanned under wet conditions at 4X and 10X magnifications using the same micro-CT scanner with a #2 source filter, at 40 kVp, and a beam hardening constant of 2. Mineral densities were determined following the referenced calibration protocol to the micro-CT scanner [13]. An average distribution of mineral densities (for both low and high-density regions) was taken over five specimens and compared to those segmented by a Gaussian curve fit to the average mineral density profile for the five specimens. Tubules were identified within stone specimens and customized MATLAB (R2013b, MathWorks Inc., Natick, MA) codes were used to analyze tubule diameter. Gaussian distributions were generated to best fit the distribution of tubule diameters and the peak of the Gaussian curve was taken as the representative tubular diameter. When the absolute difference between peak values was at least the sum of two half-widths of the half-maximum of the peaks, the tubules were considered to be of distinct structures/diameters [14].

2.3. Scanning and Transmission Electron Microscopy Techniques

After micro-CT, all specimens were embedded in LR-white resin (Electron Microscopy Sciences, Hatfield, PA), cut along the midline with a slow-speed saw, and then diamond polished. Field emission scanning electron microscopy (SEM) at 1 kilovolt (SIGMA VP500, Carl Zeiss Microscopy, Pleasanton, CA) and light microscopy (BX51, Olympus Scientific Solutions Americas Corp. Waltham, MA) techniques were performed on polished surfaces at various magnifications to make structural evaluations at multiple length scales. Proximal regions of the papilla were sectioned for transmission electron microscopy.

3. RESULTS

Representative micro-CT scan of renal pyramid specimens consistently revealed areas of mineralization at proximal and distal locations of the renal pyramid. Positive correlation was observed between proximal and distal mineralized regions; proximal minerals were identified in all cases, while distal minerals were identified only in specimens with extensive proximal mineralization. Proximal minerals were located using SEM, and were within tubular lumens (Fig 1) containing intact tubular cells with nuclei (*) as shown in figure 1a-c. Subsequently, the sectioned surface revealed mineralized regions in proximal and distal locations of the renal papilla when examined using SEM (Fig 2). In panel 2a, a mineralized tubule can be seen coursing down to the mineralizing interstitium in the distal portion of the renal papilla (detail in 2b). Tubular lumens appeared patent, despite surrounding tissues being calcified (Fig 2b, arrow heads and bracket). Further interstitial mineralization is identified in 2c, where intravascular erythrocytes (*) adjoining a nearby mineralized tubular wall can be observed. Intrafibrillar minerals within collagen fibrils of the interstitium (as opposed to intratubular) were also identified (Fig 2d). Correlation between micro-CT and electron microscopy data to extract contextual information for intratubular and interstitial minerals is reviewed in figure 3.

A micro-CT image of a representative papilla is shown in figure 3a. Proximally located minerals were often observed to exhibit a plate-like pattern of deposition in affected areas (Fig 3b). These minerals were consistently identified as intratubular in more proximal locations (Fig 3c). Distally, a mineralized tubular lumen was identified and contained spherical mineral nodules, an observation consistent with previously reported descriptions of calcified nano-particles (CNPs, Fig 3d-e) [15,16]. These particles were observed to agglutinate in the tissues surrounding distal tubules while leaving those tubule-lumens patent (Fig 3f). CNPs and agglomerated plaque were also identified in the perivascular interstitium (Fig 3g-h).

Five representative stones attached to identifiable intact stems were closely examined given that they form on a calcium phosphate deposit known as RP (Fig 4). Data from X-ray micro-CT of five stones with intact stems was volume rendered, and each stone with stem is shown in figure 4a, while virtual sections (Fig 4b) reveal the varied X-ray attenuation of the stones (darker areas) in comparison to their stems (lighter areas). Average mineral density of the stones was 711 mg/cc and stems was 1,182 mg/cc. Microarchitecture of stem-stone interface at a higher resolution as seen using an SEM is shown in figure 4c. Lower magnification electron micrographs of the stones are shown in figure 4c. Interestingly, in specimens 3–5 (Fig 4d), intact and patent tubules of diameter ranging up to 20 μm were identified within the stem of the stones, while larger tubules with a mean diameter of 65 μm were seen in all specimens using a micro-CT.

4. DISCUSSION

Fundamentally, form and function are linked. The functional unit for blood filtration in all mammalian kidneys is the nephron; it is a several centimeters long tubule of varying diameter ranging from 30–150 μm that weaves a serpentine path through regions of the

kidney that are segmented as the cortex, medulla, and papilla (with the latter two regions being the dominant functional zones within the renal pyramid) [17]. The following discussion will be within the realm of physiologic processes occurring within the nephron of the renal pyramid [18]. Many active and passive ion exchange processes occur within the nephron, and this discussion will focus on minerals that were observed in anatomy-specific regions of the renal pyramid including those commonly observed in the interstitial matrix of the papillary tip, and the tubules within this region.

The glomerulus is the site of filtration for the nephron, acting like a biological sieve separating protein and blood cells from the fluid that is to become urine. Blood passes first from the afferent arteriole and filters through the glomerulus into Bowman's capsule. The remaining blood passes into the efferent arteriole into the systemic circulation. The now uriniferous fluid passes through a variety of nephron segments which travel from the outer cortex, into the inner medulla and back repeatedly. This process takes advantage of active and passive transport of ions and a steep concentration and pressure gradients that affect different cell types and their functions. These varied regions enable concentration of solutes; the fundamental excretory product in urine. Urine first passes through the proximal convoluted tubule, leaving the cortex by passing into the medulla within the descending, thin, and ascending limbs of the loops of Henle where a steep concentration gradient in the interstitium facilitates countercurrent exchange of solutes [19]. Ultimately, the fluid enters the distal convoluted tubule before passing into the collecting duct and the renal pelvis as urine.

The uriniferous fluid initially contains a great number of solutes that are transported back into the blood to a high degree before leaving the nephron as urine. As noted above, large molecules are initially filtered at the level of the glomerulus, leaving a solution rich in glucose, sodium, chloride, potassium, and other ions. In the proximal convoluted tubule, about 60% of sodium, potassium, and calcium is resorbed along with 80% of phosphate, water, and bicarbonate, and almost 100% of glucose. Next, as the fluid passes down the descending limb loop of Henle into the papilla through a thick and thin segment, a steep interstitial concentration gradient is produced, up to 1400mOsm/kg. The principal driver of the osmotic gradient in the distal papillary interstitium is urea [18]. The thin limbs of the loops of Henle in the distal papillary region have, for years, been thought of as the site of origin of a calcium phosphate concretion known as RP [8]. In-vitro studies have calculated that within the loop of Henle, the intra-tubular fluid reaches supersaturation concentrations of calcium phosphate [20].

Solutes are transported out of the tubule and into the interstitium as the uriniferous fluid becomes increasingly hypotonic in comparison to the interstitium. The highest solute concentration is reached in the interstitial papillary tip, precisely where RP is observed. In states of dehydration, the water-impermeable collecting duct will shift to a permeable state through surface expression of aquaporin allowing reuptake of water, facilitated by this steep concentration gradient, and maintenance of total body fluid homeostasis. Charge neutrality is maintained in the papillary interstitium by virtue of ion exchange. It remains unclear, however, why phosphate deposition is favored in this region when urea is the principal driver of the concentration gradient.

Given such steep concentration gradients, physiologic stresses, and the heavy burden of the western diet on the kidney, it is a wonder that mineralization of this filtration system can be avoided at all. In individuals for whom this homeostatic mechanism becomes taxed in some way, it is conceivable that over time biominerals form. Investigations into the origin of RPs have identified small calcium deposits, herein referred to as calcified nano-particles (CNPs) throughout the renal pyramid. These particles were first noted by Anderson and Carr in the 1940s and 1950s where small mineral “droplets” were observed in a majority of specimens [5,6]. Later, Cooke identified similar mineralization within the basement membrane of the thin loops of Henle, extending into the interstitium of 43 of 62 otherwise normal kidneys [21]. Similar findings were made in 1971 by Haggitt who used transmission electron microscopy [15]. Evan and colleagues later asserted, based on sections of tissue from the very tip of the papilla, that hydroxyapatite deposits (composed of CNPs) within the basement membrane of the thin loops of Henle were the initial site of calcification in the kidney [8]. For several years after, research on the origin of nephrolithiasis largely relied on analysis of small fragments of tissue, biopsied from the very tip of the renal papilla [9,22]. It was almost eight decades later that high resolution X-ray tomography and correlative microscopy using light and electron imaging modalities have revealed and confirmed proximal calcifications as those observed by Anderson and Carr in addition to detailing micro- and ultra-structures of minerals (figures 1–3) [5–7,11]. In contrast to the proximal papilla, where minerals are often plate-like in structure, there appears to be a pattern of agglutinating CNPs in the distal papillary interstitium (Fig 2d-f).

Despite the notable anatomy-specific mineral deposits, is there a biological link between the intratubular and interstitial mineral formations and stem followed by stone formation, or are these events unlinked? Based on prior results, we contend that flow mechanics resulting from the architecture of the human renal pyramid can help explain anatomy-specific mineral formations [11]. Division of the papilla into zones 1–3, from proximal third to distal third, allowed characterization of tubule diameters and the distribution of the vasa-recta (the network of capillaries allowing countercurrent exchange). It was postulated that the effect of pressure differentials on tissue biomechanics could be described based upon Poiseuille’s law (Equation 1)$P \propto \frac{8\mu LQ}{\pi r^4}$, where pressure (P) is proportional to the dynamic viscosity of the fluid (μ), length of the tubule (L) and volumetric flowrate (Q), and inversely proportional to the fourth power of the radius (r) of the tubule. In the narrower thin limb of the loop of Henle pressure ‘P’ would increase significantly for a small change in ‘r’ as the proximal tubules collect biominerals near the walls of the tubules (where velocity of flow is significantly lower than the central-line velocity). Fundamentally, peripheral tubules (which are shorter due to the paraboloid shape of the papilla) would have proportionately lower velocity of fluid flow and would be more likely to aggregate solid debris. The aforementioned postulate was supported by the observation that microcalcifications in the more proximal and peripheral areas of zone 1 in all specimens (Fig 3a) were observed in the absence of distal interstitial RP. Additionally, there was a proportional increase in the amount of RP with increasing proximal mineralization. Given the ubiquity of proximal minerals and the apparent direct correlation between the amount of proximal minerals and the amount of RP, we contend that proximal minerals likely precede RP formation [11]. In

the present study, intact tubular cells are adjacent to proximally located plate-like minerals (Figs 1a-c, 3b-c), supporting the postulate that these calcifications are intratubular. RPs appears to be an interstitial deposit, given the patency of lumens within the distal papilla, as seen in Figure 2 as well as Figure 3d-h, consistent with prior research [8]. It is conceivable that increasing proximal mineralization could stimulate Randall's interstitial plaque.

As the concretion of calcium phosphate known as RP steadily grows, it ultimately erupts through the subsurface papillary epithelium and becomes exposed to concentrated urine in the calyx of the renal collecting system [4,9,23]. Urine, which is concentrated in uric acid and oxalates, furthers crystal growth most commonly identified as calcium and oxalate. Occasionally a proportion of uric acid or phosphate, given sufficiently aberrant pH, will precipitate [24]. As the RP is bathed in urine, the predominantly apatite surface renders itself conducive to oxalate formation resulting in steady growth of calculus [9,25]. Such calculi will often detach from the renal papilla and subsequently occlude the ureter, causing significant pain and in some cases renal failure and/or infection. Occasionally, during the surgical management of nephrolithiasis, a stone with an attached portion of RP can also be identified, herein referred to as a "stem".

In this study, five such specimens were obtained and were characterized using micro-CT and scanning electron microscopy techniques. Micro-CT revealed distinctions in mineral density between stem and stones with stones expressing heterogeneity largely by virtue of varying elemental composition [14]. Electron microscopy and micro-CT of these stems has revealed, in some cases, patent lumens of diameters equal to that of the tubules, thin loops of Henle within the renal tip (Fig 4; D3-D5). We suggest this as supporting evidence for asserting that these stems are indeed composed of RP. We have shown that, by transmission electron microscopy, RP appears to be an interstitial process and the presence of intact tubules within the stone's stems support this in accordance with previously published data [4,8,9].

Of note are some limitations to the present study. Firstly, renal pyramids were not obtained from stone forming individuals as the papilla were removed at the time of nephrectomy for renal cancer, at sites distant from the cancer which appeared anatomically normal. Stones examined did not form on the particular papillae that were studied, and are presumed to have formed on RP based on the presence of a stem like appearance and calcium phosphate region or because the surgeon plucked the specimen off of the papilla at surgery. Energy-dispersive X-ray spectroscopy data concerning the chemical composition of the plaques was performed as part of a separate study (under review) [26].

Taken together, proximal intratubular calcifications, distal interstitial calcifications, and stones with stems showing both patent tubules within calcium phosphate stems suggest a stepwise progression of events from nephrocalcinosis to nephrolithiasis (Figure 5). As the proximal tubules become occluded with the plate-like calcium-composed debris, resultant changes in fluid dynamics and diverted fluid flow will induce changes in the interstitial physiology in the distal papilla. CNPs will steadily accumulate, through an as yet un-characterized mechanism resulting in a growing deposit of apatite. When these calcifications erode through the subsurface layers of the papillary epithelium into the renal collecting system, it makes itself visible to the endoscope, and clinically is termed as Randall's plaque.

Urine continues to trickle through patent tubules of the calcified interstitium and promote the nucleation and growth of a calcium oxalate interface between stone and ‘stem’ which is a part and parcel of RP.

Previous research has viewed the interstitial CNPs to be the initial site of calcium deposition in the renal papilla [8]. In contrast, the Anderson-Carr-Randall progression (proposed in 1979 by Bruwer) views the proximal calcifications as precursors to the RP, formed through fluid transport to the distal interstitial area of the renal tip [7]. This theory is contradicted based on results from this study in which plate-like minerals were observed in the proximal renal pyramid, compared to spherical nodules in the distal papilla (Figs 3b, 3e). Given this, and that proximal minerals always exist in the presence or absence of distal minerals, we suggest that distal mineralization is a downstream process of proximal tubular occlusion with resultant changes in fluid dynamics in the paraboloid human renal pyramid. In a complex system such as the renal pyramid containing a variety of cells, ions, tubules, and matrix molecules, it is also likely that calcified nano-particles result from endocytosis and interstitial deposition by tubular cells. Given such a complex system, with very many causes prompting renal architecture-specific biominerals, the question to ask is: should pharmacological intervention be guided through an anatomy-specific targeted approach? Identification of a mineralized event in the proximal renal pyramid as the temporal precursor to distal mineralization, which can ultimately result in a symptomatic stone event, lends itself to the future development of targeted pharmacological intervention. By understanding the stepwise progression of biomineralization (intratubular -> interstitial -> plaque -> stem -> stone), we would be able to intervene well before an insoluble and painful calcium oxalate or calcium phosphate dominant stone were to develop.

Acknowledgements:

The authors thank the Biomaterials and Bioengineering Correlative Microscopy Core (http://bbcmc.ucsf.edu), UCSF for the use of MicroXCT-200 and Scanning electron microscope.

Funding Support: R21 DK109912 (SPH, MLS), NIDDK/P20DK100863 (MLS), and NIDCR/R01DE022032 (SPH)

References

1. Scales CD, Smith AC, Hanley JM, Saigal CS, Urologic Diseases in America Project CS, Project UD in A. Prevalence of kidney stones in the United States. Eur Urol. 2012 7;62(1):160–5. [PubMed: 22498635]
2. Moe OW. Kidney stones: pathophysiology and medical management. Lancet. 2006 1;367(9507): 333–44. [PubMed: 16443041]
3. Coe FL, Evan AP, Worcester EM, Lingeman JE. Three pathways for human kidney stone formation. Urol Res. 2010 6;38(3):147–60. [PubMed: 20411383]
4. Randall A the Origin and Growth of Renal Calculi. Ann Surg. 1937 6;105(6):1009–27. [PubMed: 17856988]
5. ANDERSON L, McDONALD JR. The origin, frequency, and significance of microscopic calculi in the kidney. Surg Gynecol Obstet. 1946 3;82:275–82. [PubMed: 21014137]
6. CARR RJ. A new theory on the formation of renal calculi. Br J Urol. 1954 6;26(2):105–17. [PubMed: 13172454]
7. Bruwer A Primary renal calculi: Anderson-Carr-Randall progression? AJR Am J Roentgenol. 1979 5;132(5):751–8. [PubMed: 107740]

8. Evan AP, Lingeman JE, Coe FL, Parks JH, Bledsoe SB, Shao Y, Sommer AJ, Paterson RF, Kuo RL, Grynpas M. Randall's plaque of patients with nephrolithiasis begins in basement membranes of thin loops of Henle. J Clin Invest. 2003 3 1;111(5):607–16. [PubMed: 12618515]
9. Evan AP, Coe FL, Lingeman JE, Shao Y, Sommer AJ, Bledsoe SB, Anderson JC, Worcester EM. Mechanism of formation of human calcium oxalate renal stones on Randall's plaque. Anat Rec (Hoboken). 2007 10 1;290(10):1315–23. [PubMed: 17724713]
10. Amos FF, Dai L, Kumar R, Khan SR, Gower LB. Mechanism of formation of concentrically laminated spherules: implication to Randall's plaque and stone formation. Urol Res. 2009;37:11–7. [PubMed: 19066874]
11. Hsi RS, Ramaswamy K, Ho SP, Stoller ML. The origins of urinary stone disease: upstream mineral formations initiate downstream Randall's plaque. BJU Int. 2017 1 1;119(1):177–84. [PubMed: 27306864]
12. Brauer DS, Saeki K, Hilton JF, Marshall GW, Marshall SJ. Effect of sterilization by gamma radiation on nano-mechanical properties of teeth. Dent Mater. 2008 8;24(8):1137–40. [PubMed: 18436298]
13. Djomehri SI, Candell S, Case T, Browning A, Marshall GW, Yun W, Lau SH, Webb S, Ho SP. Mineral Density Volume Gradients in Normal and Diseased Human Tissues. Aikawa E, editor. PLoS One. 2015 4 9;10(4):e0121611. [PubMed: 25856386]
14. Sherer BA, Chen L, Yang F, Ramaswamy K, Killilea DW, Hsi RS, Stoller ML, Ho SP. Heterogeneity in calcium nephrolithiasis: A materials perspective. J Mater Res. 2017 7 8;32(13): 2497–509.
15. Haggitt RC, Pitcock JA. Renal medullary calcifications: a light and electron microscopic study. J Urol. 1971 9;106(3):342–7. [PubMed: 4106437]
16. Beer MH, Porter RS, Jones TV, editors. Musculoskeletal and Connective Tissue Disorders In: The Merck Manual of Diagnosis and Therapy. 18th ed. Whitehouse Station, NJ: Wiley; 2006 p. 304.
17. Mescher AL. The Urinary System In: Junqueira's Basic Histology, 14e New York, NY: McGraw-Hill Education; 2016.
18. Lote CJ. Principles of renal physiology Fifth Edit Principles of Renal Physiology.New York, NY: Springer New York; 2013 1–204 p.
19. Pallone TL, Turner MR, Edwards A, Jamison RL. Countercurrent exchange in the renal medulla. Am J Physiol Regul Integr Comp Physiol. 2003 5 1;284(5):R1153–75. [PubMed: 12676741]
20. Asplin JR, Mandel NS, Coe FL. Evidence of calcium phosphate supersaturation in the loop of Henle. Am J Physiol. 1996 4;270(4 Pt 2):F604–13. [PubMed: 8967338]
21. Cooke SA. The site of calcification in the human renal papilla. Br J Surg. 1970 12;57(12):890–6. [PubMed: 5487030]
22. Kim SC, Coe FL, Tinmouth WW, Kuo RL, Paterson RF, Parks JH, Munch LC, Evan AP, Lingeman JE. Stone formation is proportional to papillary surface coverage by Randall's plaque. J Urol. 2005 1;173(1):117–9; discussion 119. [PubMed: 15592050]
23. Randall A Papillary Pathology as a Precursor of Primary Renal Calculus. J Urol. 1940;44(5):580–9.
24. Letavernier E, Vandermeersch S, Traxer O, Tligui M, Baud L, Ronco P, Haymann J-P, Daudon M. Demographics and characterization of 10,282 Randall plaque-related kidney stones: a new epidemic? Medicine (Baltimore). 2015 3;94(10):e566. [PubMed: 25761176]
25. Matlaga BR, Coe FL, Evan AP, Lingeman JE. The role of Randall's plaques in the pathogenesis of calcium stones. J Urol. 2007 1;177(1):31–8. [PubMed: 17161996]
26. Sherer BA, Chen L, Kang M, Shimotake AR, Wiener SV, Chi T, Stoller ML, Ho SP. A Continuum of Mineralization from Human Renal Pyramid to Stones on Stems. Under Rev.

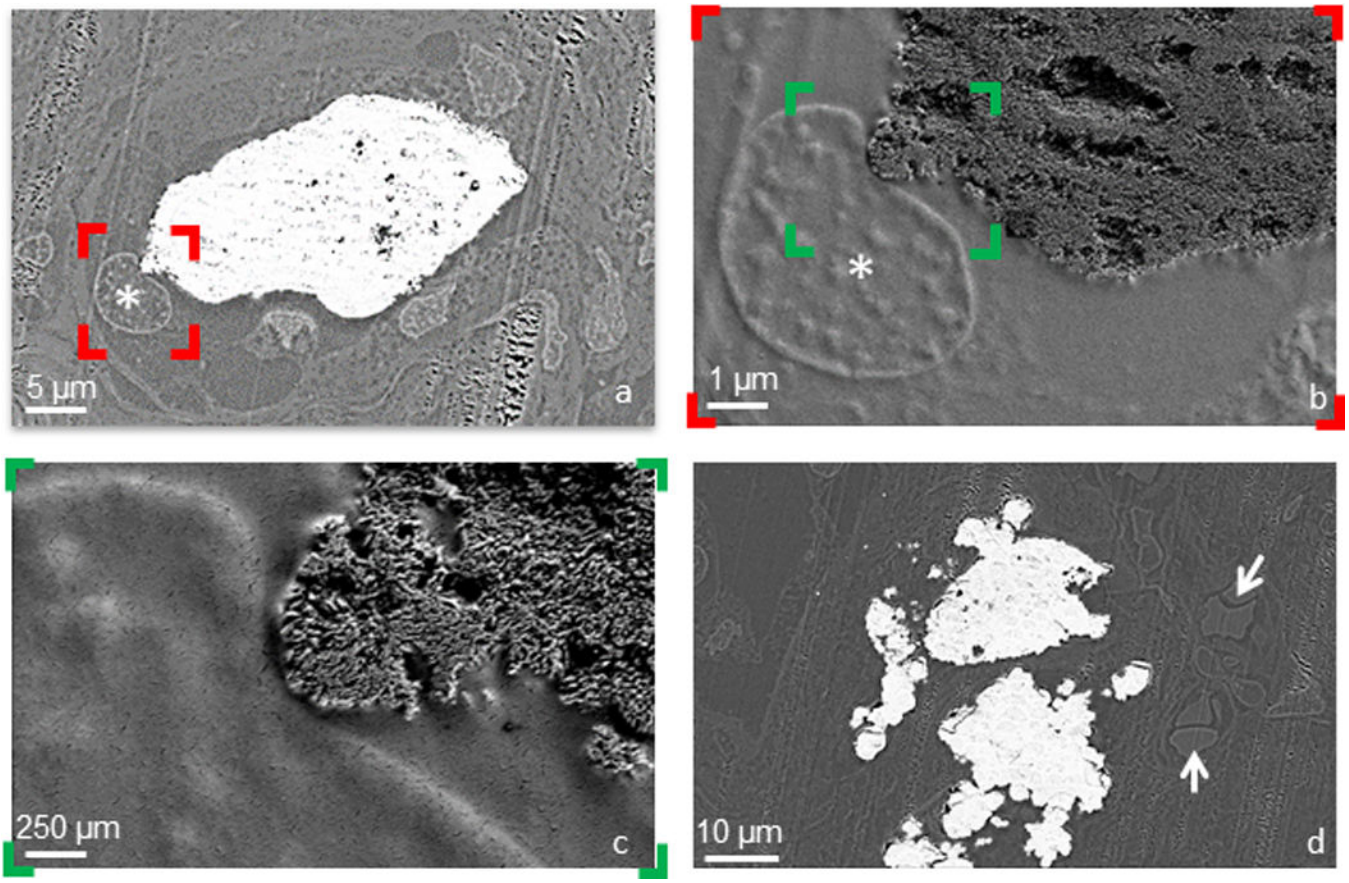

Figure 1. Intratubular mineral in the proximal regions of the papilla:
Minerals were located within tubular lumens. Occasionally, an intact tubular cell with nucleus (*) can also be seen in (a) with increasing detail as seen in (b) and (c). A representative intratubular mineral with neighboring red blood cells (arrow heads) is shown in (d).

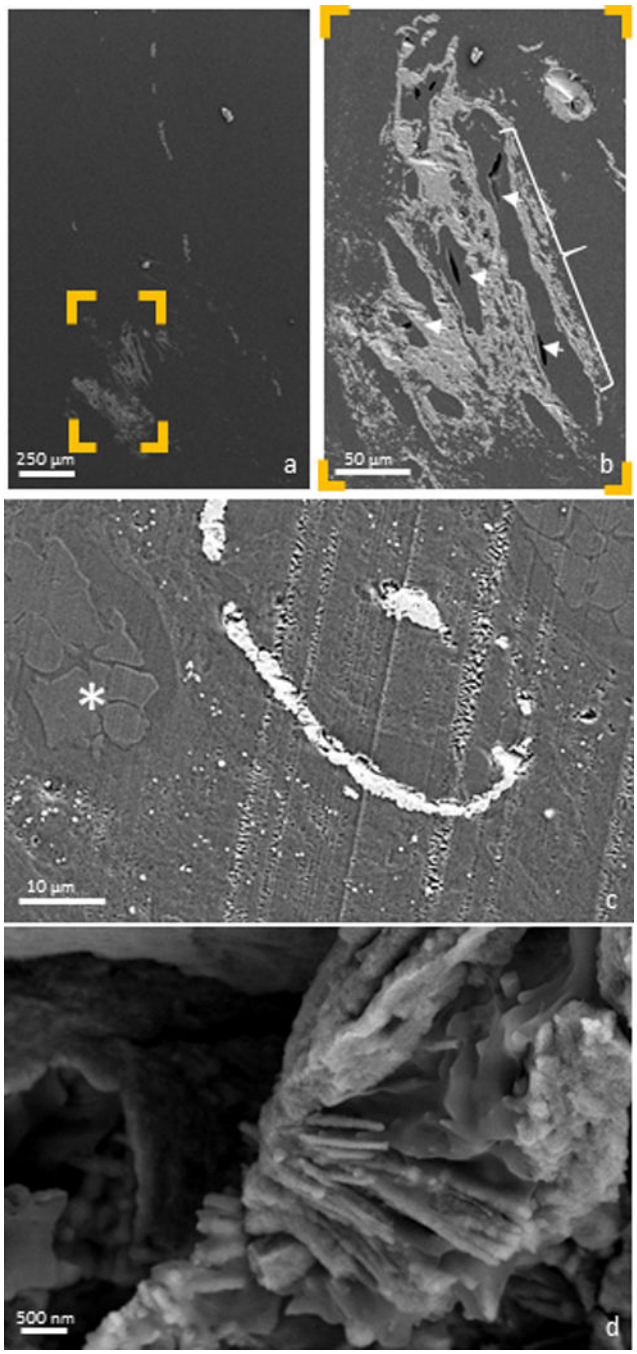

Figure 2. Examining the distal papilla:

Anatomically-specific minerals were observed by imaging the surface of an ultrasectioned distal papilla using an electron microscope. A mineralized tubule can be seen coursing distally down the entire length of the papilla in (a), with nearby mineralized interstitium shown in detail (b). Tubular lumens were patent (b, arrow heads), despite their surrounding tissues being mineralized (b, bracket). Further interstitial mineral is identified in (c), where intravascular erythrocytes (*) were observed in the adjacent mineralized tubular wall. A

mineralized collagen fibril, indicative of interstitial (as opposed to intratubular) mineralization was also identified (d).

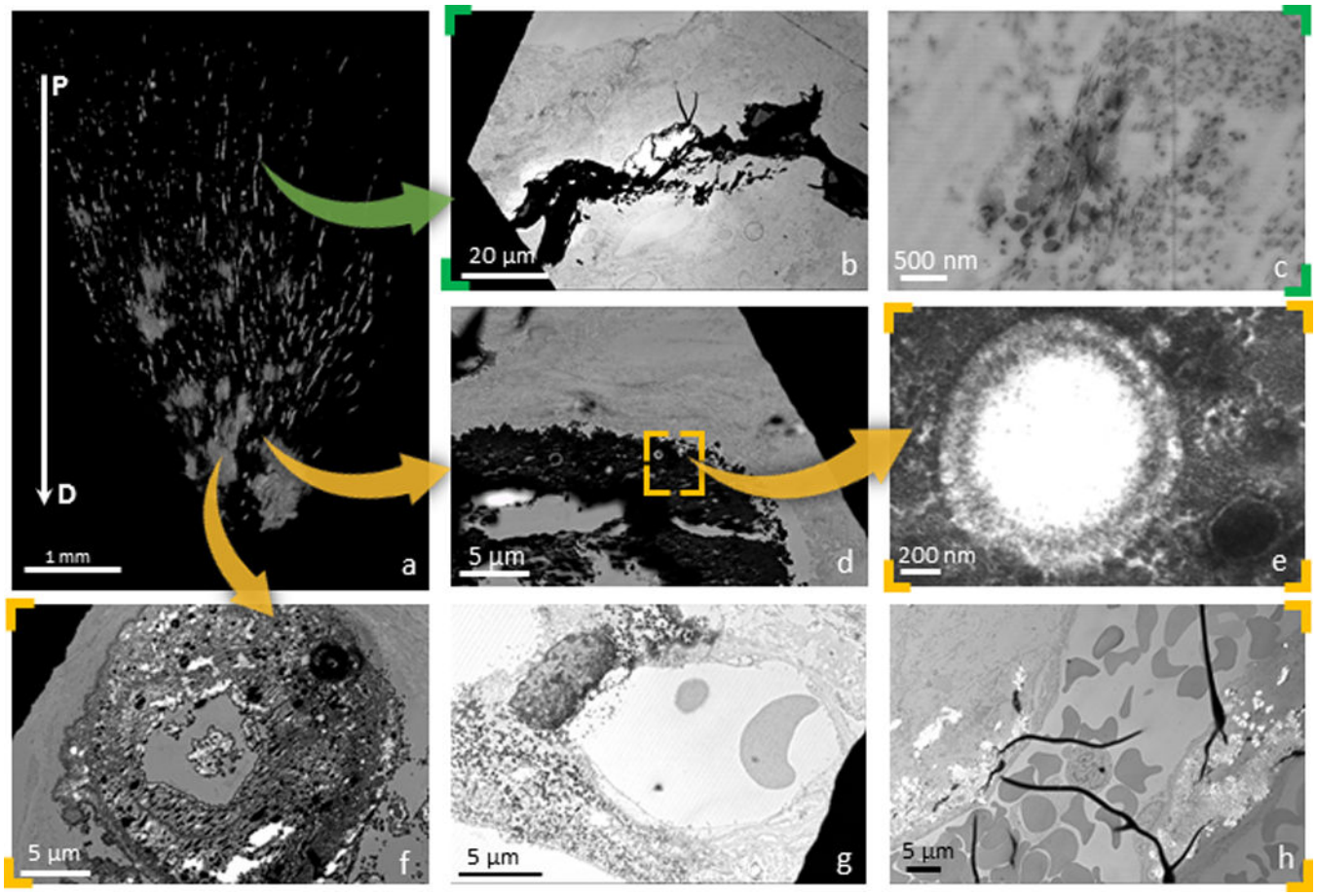

Figure 3. Correlation of data sets from X-ray micro computed tomography (micro-XCT) and scanning transmission electron microscopy (STEM) techniques:

A representative 3D volume of a human renal papilla is shown in (a). Proximal minerals were often observed to exhibit a plate-like pattern of deposition in affected areas (arrow heads denote plates) (b) and were consistently identified as intratubular (arrow heads denote tubular cell nuclei) in more proximal locations (c). Distally, mineralized tubular lumens contained spherical structures (d, detail in e). These particles were observed to agglutinate in the tissues surrounding distal tubules while leaving those tubules patent (f). Spherical particles (denoted by arrow heads) and agglomerated plaque (denoted by arrow heads) were also identified in the perivascular interstitium (g & h). P: Proximal; D: Distal

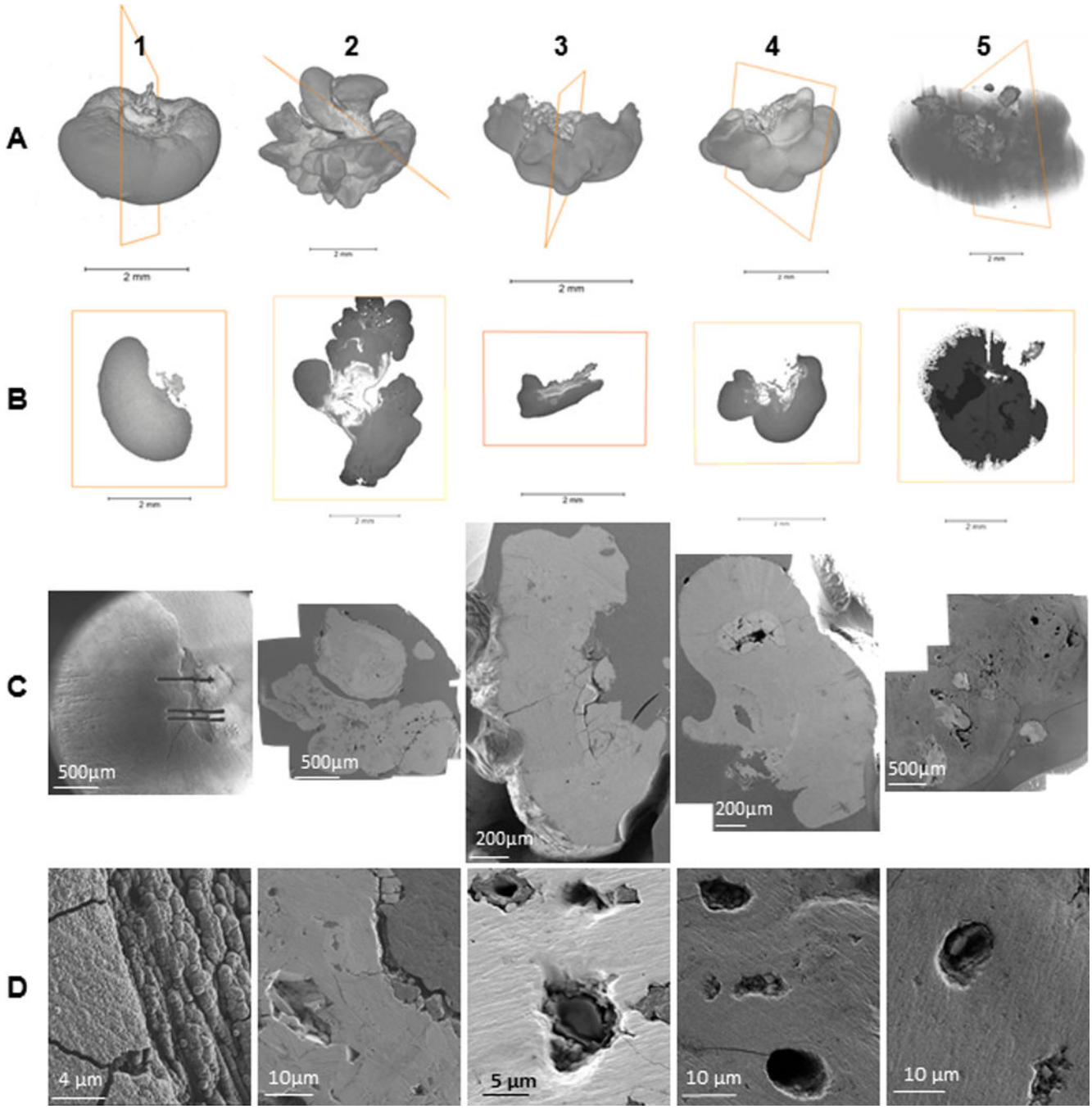

Figure 4. Examining the stem-stone interface:

Five representative stones with identifiable stems are shown. 3D volume rendered images of stone with stems are shown in (a), while cross sectional images (b) reveal the lower mineral density of the stones (darker areas) in comparison to their higher density stems (lighter areas) based on Hounsfield units. The physical cross sections of the same stones, as observed using a scanning electron microscope can be seen in (c), while at a higher magnification the detail of stone-stem interface contained within the same cross section is

shown in (d). Depending on the sectioning plane, intact and seemingly patent tubules were identified within the stem of the stone (3–5 in d).

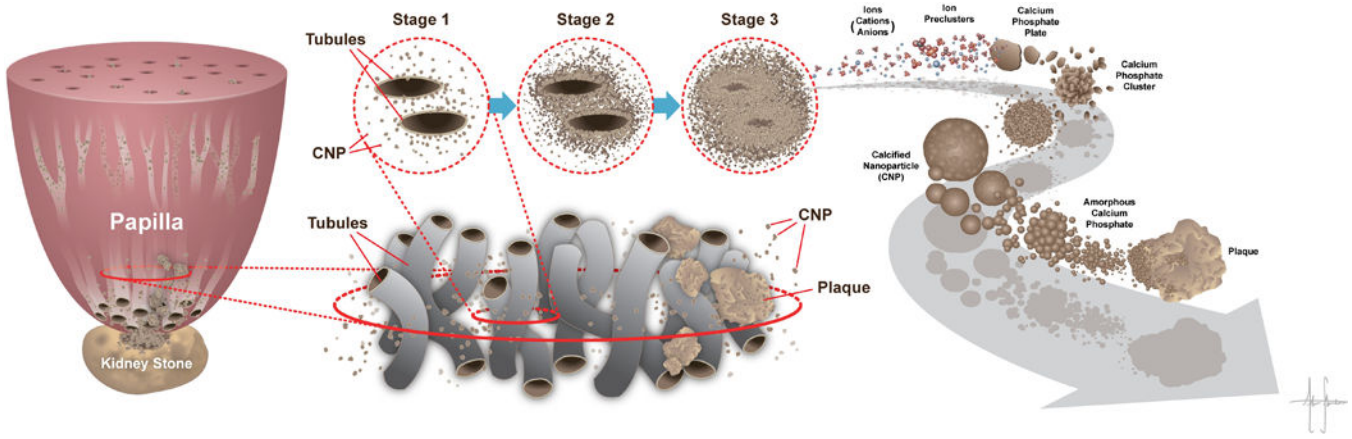

Figure 5. Model of mineral progression from proximal papilla to Randall's Plaque and a stone on a stem:

A schematic representation of a human renal papilla is presented on the left. Intratubular minerals can be seen within the top portion of the papilla. As ions coalesce to form pre-clusters and calcified nanoparticles (CNPs), they subsequently agglomerate into higher ordered calcium phosphate phases such as amorphous calcium phosphate (Stages 1–3 plus rightward progression). Amorphous calcium phosphate will eventually form fully developed Randall's plaque (bottom left and center). Randall's plaque (stage 3) erodes through the subsurface layers of the papillary tip to form a stem, and serves as the nucleator of stone growth in the urinary space (bottom left). Note: Schematic not drawn to scale.